

ARTICLE

Received 20 Oct 2015 | Accepted 24 Nov 2015 | Published 5 Jan 2016

DOI: 10.1038/ncomms10281

OPEN

Stepwise B-cell-dependent expansion of T helper clonotypes diversifies the T-cell response

Julia Merckenschlager¹, Mickaël J. Ploquin^{1,†}, Urszula Eksmond¹, Rakieb Andargachew², Georgina Thorborn^{1,†}, Andrew Filby^{1,†}, Marion Pepper³, Brian Evavold² & George Kassiotis^{1,4}

Antigen receptor diversity underpins adaptive immunity by providing the ground for clonal selection of lymphocytes with the appropriate antigen reactivity. Current models attribute T cell clonal selection during the immune response to T-cell receptor (TCR) affinity for either foreign or self peptides. Here, we report that clonal selection of CD4⁺ T cells is also extrinsically regulated by B cells. In response to viral infection, the antigen-specific TCR repertoire is progressively diversified by staggered clonotypic expansion, according to functional avidity, which correlates with self-reactivity. Clonal expansion of lower-avidity T-cell clonotypes depends on availability of MHC II-expressing B cells, in turn influenced by B-cell activation. B cells clonotypically diversify the CD4⁺ T-cell response also to vaccination or tumour challenge, revealing a common effect.

¹Retroviral Immunology, The Francis Crick Institute, Mill Hill Laboratory, London NW7 1AA, UK. ²Department of Microbiology and Immunology, Emory University School of Medicine, Atlanta, Georgia 30322, USA. ³Department of Immunology, University of Washington, Seattle, Washington 98109-8059, USA. ⁴Department of Medicine, Faculty of Medicine, Imperial College London, London W2 1PG, UK. † Present addresses: Institut Pasteur, Unité HIV Inflammation et Persistance, Paris 75015, France (M.J.P.); William Harvey Research Institute, Queen Mary University of London, London EC1M 6BQ, UK (G.T.); Faculty of Medical Sciences, Newcastle University, Newcastle upon Tyne NE1 7RU, UK (A.F.). Correspondence and requests for materials should be addressed to G.K. (email: george.kassiotis@crick.ac.uk).

Adaptive immunity relies on clonal expansion and retention of antigen-specific lymphocytes bearing somatically generated and selected antigen receptors. Selection for lymphocytes with particular T-cell or B-cell receptors (TCRs and BCRs, respectively) occurs throughout the different stages of lymphocyte development, effector response and memory formation, based on thresholds of affinity for self or foreign antigen^{1–4}. For example, the strength of TCR signalling is responsible for the selective advantage of high-affinity clonotypes that commonly dominate the peak CD4⁺ T-cell response^{5–9}.

The selective forces driving the dominance of high-affinity CD4⁺ T cells during priming may continue to operate during memory formation. However, the relationship between primary expansion of a clonotype and memory formation is not always predictable. Indeed, the potential of distinct TCR clonotypes to form memory following LCMV infection does not correspond to the degree of their primary expansion⁹. Furthermore, comparison of two CD4⁺ T clones responding to *Listeria monocytogenes* infection revealed inverse behaviour during primary and secondary responses¹⁰, which is linked to avidity for self rather than foreign antigen, setting intrinsic thresholds for sensitivity and responsiveness¹¹. The strength of self-reactivity, reflected in the expression levels of CD5, was also proposed as a clonotype-specific property directly related to the strength of TCR signalling in the response of several monoclonal or polyclonal CD4⁺ T cells to foreign antigen¹². Moreover, individual CD4⁺ T cells bearing identical TCRs differ considerably in their ability to expand and differentiate in response to *L. monocytogenes* infection¹³, highlighting the influence of stochastic events, not linked to TCR affinity. In addition, the ratio of high- and low-affinity CD4⁺ T cells in response to vaccination is heavily influenced by the co-administered adjuvant¹⁴, the use of peptide instead of protein antigens¹⁵, the nature of the vaccine vector¹⁶ or simply by antigen dose^{17,18}. Despite the potential of T-cell-extrinsic factors to influence the clonotypic composition of a T-cell response, their mechanism of action or amplitude are not yet fully understood.

Here, we used a well-characterized model to study the clonotypic evolution of the CD4⁺ T-cell response to retroviral infection. Inoculation of C57BL/6 (B6) mice with Friend virus (FV), a retroviral complex of Friend murine leukaemia virus (F-MLV) and spleen focus-forming virus (SFFV), causes protracted infection with several weeks of viral replication^{19,20}. We have previously described a TCR β -transgenic strain, which generates diverse CD4⁺ T-cell clonotypes with a range of functional avidities for the dominant H2-A^b-restricted env_{122–141} epitope within the surface unit of the F-MLV *env* gene^{8,21}. Our results revealed that the CD4⁺ T-cell clonotypic hierarchy, set early in the response and determined by TCR avidity, can be reversed later in infection. This pattern of clonotypic progression is created by asynchronous expansion of distinct CD4⁺ T-cell clonotypes, according to antigen reactivity. Importantly, CD4⁺ T-cell clonotypic progression relies on B-cell activation and antigen presentation. Thus, not only is the B-cell response to infection helped and clonally diversified by CD4⁺ T cells, it also reciprocally helps and clonally diversifies the CD4⁺ T-cell response.

Results

Diversity of virus-specific CD4⁺ T cells increases over time.

To study the clonotypic composition of an antiviral CD4⁺ T-cell response, we used infection of wild-type (WT) B6 mice with FV. To unequivocally identify a cohort of virus-specific CD4⁺ T cells over the course of infection, we used an adoptive transfer

system²². Mice received allotypically marked EF4.1 T CR β -transgenic CD4⁺ T cells (~10,000 virus-specific cells engrafted per mouse), at the time of infection. The use of endogenous TCR α chains in EF4.1 T cells generate a semi-polyclonal TCR repertoire enriched in clonotypes reactive with the F-MLV env_{122–141} epitope²¹. Importantly, pairing of the transgenic TCR β chain with TCR V α 2 chains (encoded by *Trav14* gene segments) or V α 3 chains (encoded by *Trav9* gene segments) creates clonotypes with higher or lower functional avidity, respectively^{21,23}.

Numbers of virus-specific donor CD4⁺ T cells exhibited typical expansion and contraction kinetics (Fig. 1a). As previously observed⁸, the peak response was homogeneously dominated by high-avidity clonotypes, with V α 2 clonotypes rising to >75% on day 7 of infection (Fig. 1b). Notably, however, during progression of the response, the frequency of V α 2 clonotypes declined, on average, but varied wildly (5–95%) between identically treated individual hosts (Fig. 1b).

Although, at the population level, V α 2 clonotypes display higher functional avidity than V α 3 clonotypes, there exists the potential for considerable diversity in the semi-polyclonal repertoire of EF4.1 T cells^{21,23}. To examine whether the observed changes in clonotypic composition were indeed caused by differences in TCR avidity between clonotypes, we measured the frequency of unique TCR clonotypes, by deep-sequencing the endogenous *Tcra* chains in virus-specific EF4.1 CD4⁺ T cells. Using *Tcra*^{+/-} EF4.1 CD4⁺ T cells, we first confirmed that replacement of V α 2 clonotypes during FV infection was not owing to potential expression of a second TCR α chain (Supplementary Fig. 1). Grouping clones into clonotypes sharing identical amino acid sequences, revealed that the peak (day 7) virus-specific V α 2 response was overwhelmingly (~90%) dominated by a single clonotype (indicated by red color; CDR3 sequence CAAITGNTGKLIIF) in all mice (Fig. 1c). This clonotype was the single largest in the entire virus-specific and non-specific V α 2 preimmune repertoire (Fig. 1c). The frequency of this dominant clonotype remained high (>60%) within virus-specific V α 2 cells throughout infection, although it was slightly reduced in comparison with its peak, and additional clonotypes were also visible at later time points (Fig. 1c). In contrast, V α 3 cells were considerably more polyclonal (Fig. 1c). The peak of the virus-specific V α 3 response in all mice examined was also dominated by a single clonotype (indicated in red color; CDR3 sequence CVLSGDYSNNRLTL), which however, comprised only ~55% of V α 3 cells on day 7 and significantly less (between 7 and 46% in individual mice) at later time points (Fig. 1c). This particular clonotype was rare (<0.5%) in the preimmune repertoire (Fig. 1c). Notably, the virus-specific V α 3 response was also characterized by two other groups of clonotypes that exhibited distinct kinetics. The first group comprised of only two ‘public’ clonotypes (indicated by green colours; CDR3 sequences CALDNTNTGKLTFF and CALNVGDNSKLIW), which together made ~10% of all virus-specific V α 3 cells, a frequency that remained remarkably stable throughout the course of infection (Fig. 1c). The second group comprised of several (>12) distinct clonotypes (indicated by blue-purple colours), all sharing the SNNRIFF motif in their CDR3 sequences, created by the use of the *Traj31* segment (Fig. 1c). The latter group contained clonotypes that were not always shared between separate mice, but collectively increased in frequency to 30–50% of the virus-specific V α 3 cells by day 49 of infection (Fig. 1c). Thus, the clonotypic diversity of virus-specific EF4.1 CD4⁺ T cells increased over time owing to the decrease in the proportion of initially dominant V α 2 clonotypes in the overall response, and increase in the representation of *Traj31*-using clonotypes within the V α 3 response.

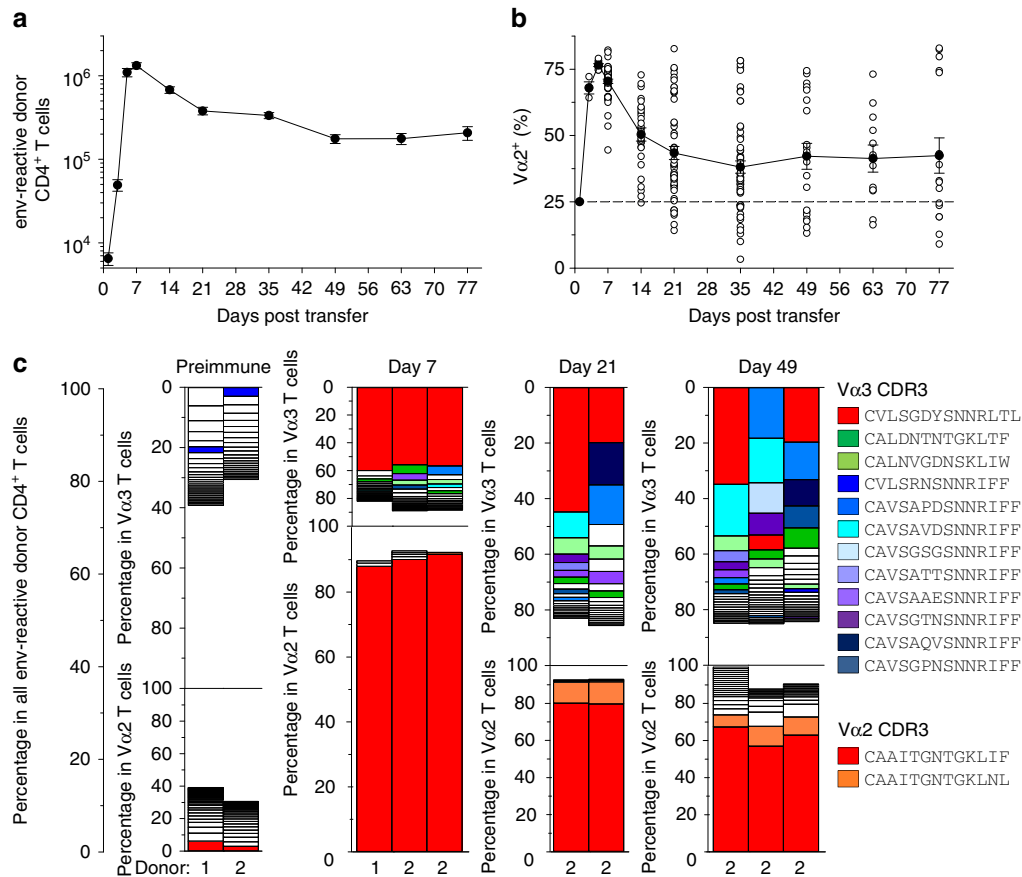


Figure 1 | Clonotypic diversity of virus-specific CD4⁺ T cells increases over the course of FV infection. (a) Absolute numbers and (b) V α composition of env-reactive donor EF4.1 CD4⁺ T cells in the spleens of recipient mice after adoptive T-cell transfer and FV infection ($n=9-61$ mice per time point; $P<0.001$ between V α 2 frequency on day 7 and any later time point, Mann-Whitney rank sum test). (c) Frequency of various V α 2 and V α 3 clonotypes in total EF4.1 CD4⁺ T cells from two uninfected donor mice (preimmune; donors 1 and 2) or in env-reactive EF4.1 CD4⁺ T cells from the spleens of recipient mice after adoptive T-cell transfer from the indicated donor and FV infection. Each bar graph represents an individual mouse. Clonotypes with frequencies <0.5% are not plotted for simplicity. Identical clonotypes within V α 2 and V α 3 subsets are marked with the same color, with red color indicating the dominant V α 2 and V α 3 clonotypes. The scale of the V α 2 and V α 3 plots are adjusted to the relative ratio of the two subsets at a given time point.

Clonotypic behaviour correlates with self-reactivity. Our previous studies indicated lower functional avidity for viral antigen in V α 3 than in V α 2 clonotypes^{21,23}, but were limited to the bulk V α 2 and V α 3 populations. To further investigate differences between unique clonotypes using more accurate measures of TCR affinity, we used hybridoma cell lines representing the two major types of behaviour during the response, ‘red’ V α 2 and *Traj31*-using ‘blue-purple’ V α 3 (Fig. 2a). These clones were comparably abundant in the preimmune repertoire of EF4.1 mice (Fig. 1c, preimmune) and exemplified the behaviour of other similar clones (Fig. 1c).

The two clones expressed comparable TCR levels (Fig. 2a) and their stimulation with env peptide *in vitro* reproduced the difference in functional avidity between the bulk V α 2 and V α 3 populations (Fig. 2b). Surprisingly, however, the functional avidity of these two clones correlated weakly with binding affinity of the TCR to env pMHC complexes (Fig. 2c). Moreover, precise measurement of two-dimensional TCR affinity for A^b-env₁₂₅₋₁₃₅ using a micropipette adhesion frequency assay^{24,25}, revealed only minor differences in effective TCR affinities between the two clones (Fig. 2d).

In addition to TCR affinity for antigen, self-reactivity has recently been shown to strongly influence the sensitivity of CD4⁺ T cells to antigenic stimulation^{11,12}. Therefore, we examined if differences in functional avidity between the

selected V α 2 and V α 3 clones reflected differences in self-reactivity. The genes encoding the TCR α chains of these two clones were used to generate two TCR $\alpha\beta$ doubly transgenic mouse strains (referred to as EV α 2 and EV α 3, respectively) also expressing the same TCR β as the TCR β -transgenic EF4.1 mice. T-cell development proceeded normally in both EV α 2 and EV α 3 mice, but was considerably more efficient in the former (Fig. 2e,f). Indeed, although total thymocyte numbers were near-normal in both monoclonal TCR-transgenic strains, the frequency and absolute number CD4 single-positive thymocytes was significantly higher in EV α 2 mice (Fig. 2e,f), indicating more efficient positive selection. Consistent with this notion, levels of CD5, which correlate with the strength of self-reactivity, were significantly higher in EV α 2 than in EV α 3 post-selection (CD4⁺CD8⁻TCR^{high}) thymocytes (Fig. 2g). In comparison with cells from the parental EF4.1 strain, which expressed normal CD5 levels (Supplementary Fig. 2a), EV α 2 and EV α 3 thymocytes expressed 63 and 34%, respectively, of normal CD5 levels. Peripheral CD4⁺ T-cell numbers, which also reflect the degree of self-reactivity²⁶, were comparable to the WT levels in EV α 2 mice, but significantly reduced in EV α 3 mice (Supplementary Fig. 2b). Mature CD4⁺ T cells were homogeneously naive (CD44^{low}CD25⁻) in both monoclonal TCR-transgenic strains and expressed comparable TCR levels (Supplementary Fig. 2c). CD5 levels were reduced in both EV α 2

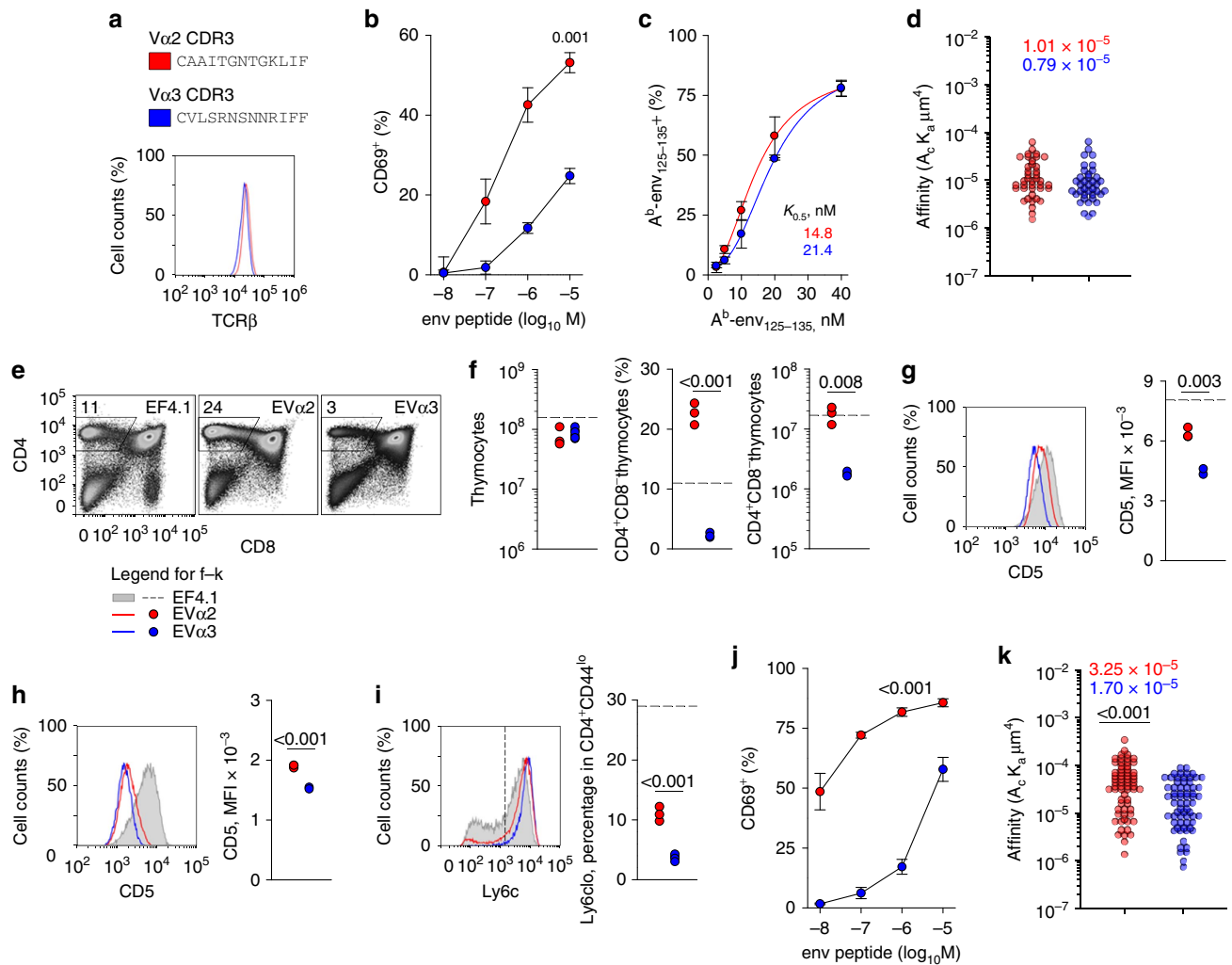


Figure 2 | Development and reactivity with self and foreign antigen of monoclonal EVα2 and EVα3 T cells. (a) CDR3 sequences and TCRβ expression levels in two hybridoma cells lines representing the indicated clonotypes. (b) Responsiveness of the same hybridoma cells lines as in a to overnight stimulation with env₁₂₂₋₁₄₁ peptide, measured by CD69 upregulation ($n=2$). (c) Frequency of A^b-env₁₂₅₋₁₃₅ tetramer-positive cells, at different tetramer concentration, following staining of the same hybridoma cells lines as in a and normalized for TCR expression. Symbols represent the means (\pm s.e.m., $n=2$) of experimental data, whereas lines are fits using a four-parameter Hill equation. Numbers next to the regression lines denote apparent affinity ($K_{0.5}$) estimates. (d) Effective two-dimensional TCR affinities for A^b-env₁₂₅₋₁₃₅ of T-cell hybridomas measured by the micropipette adhesion frequency assay and normalized by TCR surface density. Each individual data point represents the affinity of a single T cell. Numbers in the plot represent the effective affinity geometric mean of the population. (e) Flow cytometric analysis of thymocyte development in EF4.1, EVα2 and EVα3 TCR-transgenic mice. (f) Absolute number of total thymocytes and frequency and number of CD4 single-positive thymocytes in the same mice as in e. (g) CD5 levels in post-selection (CD4⁺CD8⁻TCR^{high}) thymocytes from the same mice as in e. (h) CD5 levels in naive splenic CD4⁺ T cells from EVα2 and EVα3 mice. (i) Ly6c levels in naive splenic CD4⁺ T cells from the same mice. In f-i, each symbol represents an individual mouse from one representative of two experiments. Horizontal dashed lines represent the mean values for control EF4.1 mice. (j) Responsiveness of EVα2 and EVα3 T cells to overnight env₁₂₄₋₁₃₈ peptide stimulation. Responses were measured by CD69 upregulation and are plotted as means (\pm s.e.m., $n=3-4$). (k) Effective two-dimensional TCR affinities for A^b-env₁₂₅₋₁₃₅ of primary T cells measured by the micropipette adhesion frequency assay and normalized by TCR surface density, and plotted as described in d.

and EVα3 peripheral T cell in comparison with thymocytes and with WT T cells (Fig. 2h). This was likely because of the relative paucity of MHC II-expressing cells in the periphery of these B-cell-deficient *Rag1*^{-/-} EVα2 and EVα3 mice. Indeed, comparison of EVα2 T cells from B-cell-deficient *Rag1*^{-/-} or B-cell-sufficient *Rag1*^{+/+} mice revealed a specific role for B cells in maintaining CD5 levels in peripheral, but not thymic CD4⁺ T cells (Supplementary Fig. 2d,e). Nevertheless, CD5 levels remained significantly higher in EVα2 than in EVα3 peripheral T cells (Fig. 2h) and loss of Ly6C expression, which signifies higher self-reactivity²⁷, marked a higher proportion of

EVα2 than in EVα3 peripheral T cells (Fig. 2i). Phenotypic differences between monoclonal EVα2 and EVα3 T cells correlated remarkably well with functional avidity, which was reflected in their sensitivity to *in vitro* env peptide stimulation (Fig. 2j). In contrast, two-dimensional TCR affinity for A^b-env₁₂₅₋₁₃₅ differed only by a factor of two between the two clones (Fig. 2k). Although this difference was statistically significant, it was too small to account for the disparity in antigen reactivity. Thus, functional avidity of EVα2 and EVα3 T cells better correlated with self-reactivity than with affinity for antigen.

T-cell clonal composition depends on infection kinetics. In B6 mice, acute FV infection is followed by chronic low-level infection, which can be ultimately cleared with kinetics that likely differ most significantly between FV-infected hosts. An effect of viral load on clonotypic composition was suggested by a strong correlation between F-MLV DNA copy numbers in the spleens of FV-infected recipients and frequency of V α 2 clonotypes in virus-specific CD4⁺ T cells 35 days post infection (Fig. 3a). However, this positive correlation (Fig. 3a) argued against relative loss of V α 2 clonotypes owing to excessive activation, as suggested by studies in another TCR-transgenic system^{10,11}. To examine whether viral load directly determined the clonotypic composition of the antiviral T-cell response, we infected adult B6 mice with N-tropic F-MLV (F-MLV-N), which is restricted by

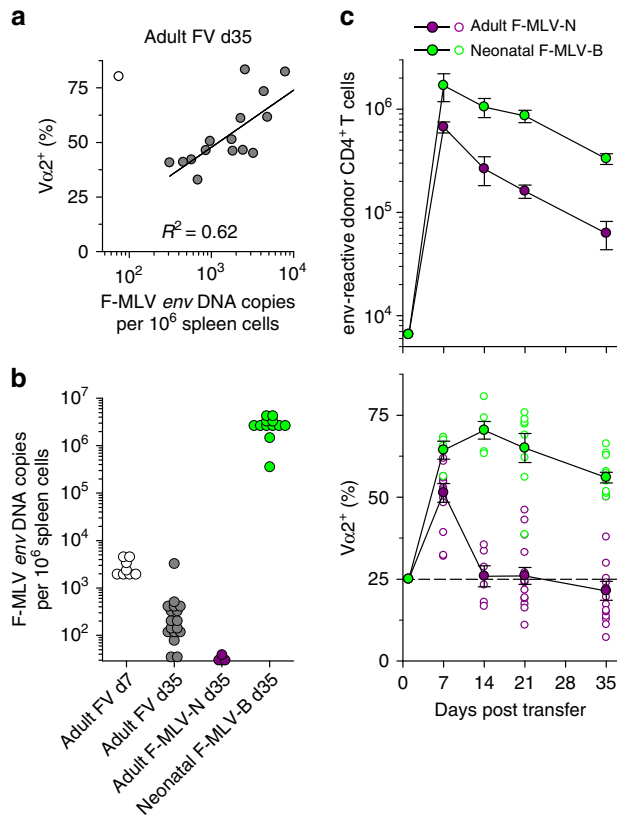


Figure 3 | Effect of infection kinetics on the clonal composition of virus-specific CD4⁺ T cells. (a) Frequency of V α 2⁺ cells within env-reactive donor EF4.1 CD4⁺ T cells plotted against copies of F-MLV env DNA in the spleens of recipient mice 35 days after adoptive T-cell transfer and FV infection. Symbols represent individual mice. The mouse represented with an open symbol was excluded from the regression analysis. (b) Copies of F-MLV env DNA in the spleens of recipient mice that were infected as adults with FV or F-MLV-N or as neonates with F-MLV-B. All recipients received EF4.1 CD4⁺ T cells as adults and analysed at the indicated time point after T-cell transfer. Each symbol is an individual mouse. The dashed line denotes the detection limit. (c) Absolute numbers (top) and V α composition (bottom) of env-reactive donor EF4.1 CD4⁺ T cells in the spleens of recipient mice after T-cell adoptive transfer in adult mice either infected with F-MLV-N at the time of T-cell transfer or with F-MLV-B as neonates ($n = 4$ –15 mice per time point; $P < 0.001$ between the two types of host on days 14–35, Mann-Whitney rank sum test). Closed symbols are the means (\pm s.e.m.); open symbols are individual mice; the dashed line represents the frequency of V α 2⁺ cells in preimmune env-reactive EF4.1 CD4⁺ T cells.

the product of the *Fv1^b* allele and quickly eliminated from these mice²⁸ (Fig. 3b). In addition, we infected neonatal B6 mice with B-tropic F-MLV (F-MLV-B), which results in life-long high-level infection (Fig. 3b) and used them 6–8 weeks later as T-cell hosts. The magnitude of the EF4.1 CD4⁺ T-cell response to adult F-MLV-N or neonatal F-MLV-B infection was proportional to the degree of viral replication in these two infections (Fig. 3c). However, the frequency of V α 2 clonotypes in virus-specific donor CD4⁺ T cells declined quickly and homogeneously in all recipients transiently infected with F-MLV-N, whereas it remained very high in all recipients with non-resolving F-MLV-B infection (Fig. 3c). These results demonstrated that the clonotypic evolution of the EF4.1 CD4⁺ T-cell response to retroviral infection was directly determined by the kinetics of viral replication and that higher antigen levels promoted, rather than hindered, clonotypes with higher antigen sensitivity.

B cells mediate clonal replacement in CD4⁺ T cells. T cells recognize viral antigens only through APCs. Thus, we reasoned that the effect of viral antigen availability on the composition virus-specific CD4⁺ T cells involved APCs. In addition to acting as APCs to T cells, B cells mount their own antigen-specific and non-specific response to viral infection with distinct temporal kinetics. In response to FV infection, the frequency of germinal center CD38^{lo}GL7^{hi} cells within IgD^{lo}CD19⁺ B cells slowly increased starting from day 10 post infection and continuing until the last time point studied (day 35; Fig. 4a,b). Interestingly, the rise in activated B cells temporally matched the decline in V α 2 clonotypes in virus-specific donor CD4⁺ T cells in FV infection (Fig. 1b and Fig. 4a). To examine a possible link, we compared hosts infected with FV with those coinfecting with FV and lactate dehydrogenase-elevating virus (LDV), which has been previously shown to induce rapid polyclonal B-cell activation and enhance FV replication²⁹. As expected, FV-LDV coinfection greatly accelerated the rise in germinal center B cells and induced higher expression of MHC II on all B cells (Fig. 4a,c). Importantly, FV-LDV coinfection resulted in significantly faster decline in the frequency of V α 2 clonotypes in virus-specific EF4.1 CD4⁺ T cells, than FV infection (Fig. 4d), supporting a role for polyclonally activated B cells.

As coinfection with LDV is likely to affect multiple processes during the response to FV, we next examined if the accelerated V α 2 clonotype decline required T cell–B cell interaction. To this end, we used EF4.1 CD4⁺ T cells deficient in *Sh2d1a* (encoding SAP, multiple signalling lymphocyte activation molecule-associated protein), which is required for prolonged CD4⁺ T cell–B cell contacts³⁰. Although SAP deficiency in donor CD4⁺ T cells had little effect on their numerical response to FV infection or FV-LDV coinfection, it completely negated the accelerated decline of V α 2 clonotypes in virus-specific EF4.1 CD4⁺ T cells by LDV (Fig. 4d).

As T-cell-specific SAP deficiency shortens, but does not abolish T cell–B cell interaction³⁰, we next used mice deficient in B cells (*Ighm*^{−/−}) as hosts. In the complete absence of B cells, high-avidity V α 2 clonotypes were induced and maintained at high levels throughout FV infection or FV-LDV coinfection (Fig. 4e). To dissociate a possible effect of B cells as APCs from other B-cell-dependent processes in the host (for example, splenic structure) we reconstituted non-irradiated *Ighm*^{−/−} hosts with either MHC II-sufficient or -deficient B cells (Supplementary Fig. 3). Following FV-LDV coinfection, MHC II-sufficient, but not -deficient B cells significantly reduced the frequency of high-avidity V α 2 clonotypes, in a dose-dependent manner, without affecting the total virus-specific donor CD4⁺ T-cell numbers (Fig. 4f). Therefore, clonotypic replacement of V α 2 virus-specific

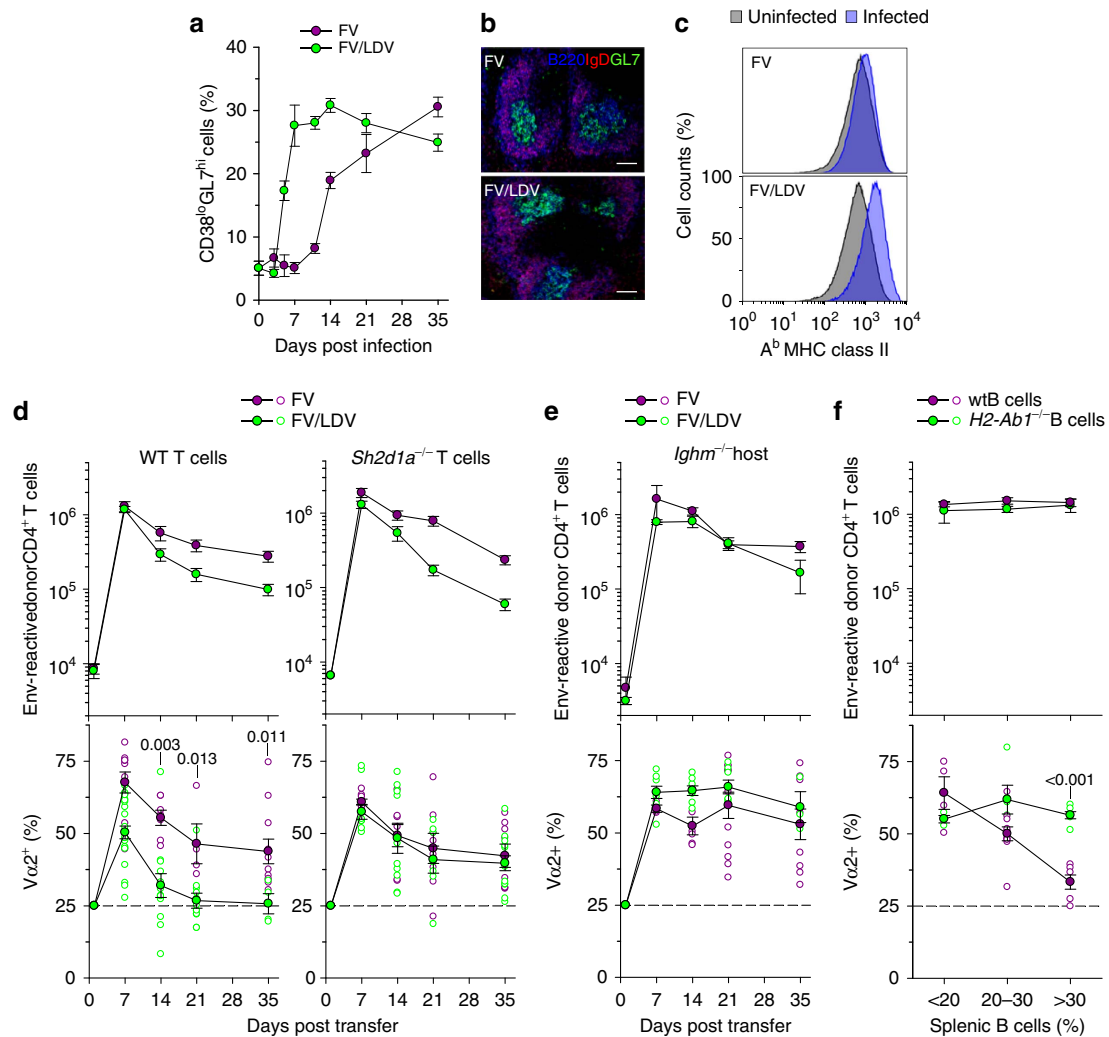


Figure 4 | Clonal replacement in virus-specific CD4⁺ T cells requires cognate B-cell interaction. (a) Frequency of germinal center-phenotype (CD38^{lo}GL7^{hi}) cells in CD19⁺IgD^{lo} splenic B cells over the course of FV infection or FV/LDV coinfection ($n = 4-13$; $P < 0.002$ between the two infections on days 5-14, Mann-Whitney rank sum test). (b) Germinal center (B220⁺IgD⁻GL7⁺) presence in the spleen of the same mice in **a** 35 days post infection. The scale bar is 250 μm . (c) MHC II expression in B220⁺CD19⁺ B cells from the spleen of the same mice in **a** 7 days post infection, compared with uninfected mice. ($P = 0.0016$ between the two infections, Student's t -test). (d) Absolute numbers (top) and V α composition (bottom) of WT (left) or *Sh2d1a*^{-/-} (right) env-reactive donor EF4.1 CD4⁺ T cells in the spleens of recipient mice after adoptive T-cell transfer and FV infection ($n = 3-8$ mice per time point) or FV/LDV coinfection ($n = 3-9$ mice per time point). (e) Absolute numbers (top) and V α composition (bottom) of env-reactive donor EF4.1 CD4⁺ T cells in the spleens of WT or *Ighm*^{-/-} recipient mice after adoptive T-cell transfer and FV infection ($n = 4-11$ mice per time point) or FV/LDV coinfection ($n = 4-23$ mice per time point). (f) Absolute numbers (top) and V α composition (bottom) of env-reactive donor EF4.1 CD4⁺ T cells in the spleens of *Ighm*^{-/-} mice previously reconstituted with WT ($n = 18$) or *H2-Ab1*^{-/-} B cells ($n = 14$) 14 days after adoptive T-cell transfer FV/LDV coinfection, plotted against the level of B-cell reconstitution. In **d-f**, closed symbols are the means (\pm s.e.m.); open symbols are individual mice.

CD4⁺ T cells over the course of infection required cognate T cell-B cell interaction.

CD4⁺ T-cell clonal replacement affects all Th subsets. Follicular helper (Tfh) cells rely on B-cell interaction and the germinal center response for their differentiation and persistence. Thus, it was theoretically possible that B cells promoted Tfh differentiation of particular T-cell clonotypes selectively, whose representation was subsequently proportional to the magnitude of the germinal center response. To test the requirement for the physical germinal center structures, we used *Tnfrsf1a*-deficient hosts, which show incomplete segregation of T-cell and B-cell areas in secondary lymphoid organs and are unable to mount a germinal center response (Fig. 5a,b). In comparison with those in

WT hosts, higher numbers of virus-specific donor CD4⁺ T cells were recovered from *Tnfrsf1a*-deficient hosts throughout the response (Fig. 5c). Importantly, however, the V α 2 and V α 3 composition of donor CD4⁺ T cells was comparable between the two types of hosts (Fig. 5c), ruling out a requirement for germinal centres in the clonotypic evolution of virus-specific CD4⁺ T cells.

To directly examine if replacement of V α 2 clonotypes was owing to preferential differentiation into Tfh cells, we conditionally ablated *Bcl6* in donor CD4⁺ T cells, precluding their Tfh differentiation. EF4.1 CD4⁺ T cells were isolated from mice carrying a Cre-conditional *Bcl6* (*Bcl6*^C) and a YFP reporter (*Gt(ROSA)26Sor*^{YFP}) allele and also expressed Cre under the control of the *Tnfrsf4* promoter (*Tnfrsf4*^{Cre}), thus initiating YFP expression and *Bcl6* deletion only upon T-cell activation³¹ (Fig. 5d,e). EF4.1 CD4⁺ T cells with either WT or *Bcl6*^C alleles,

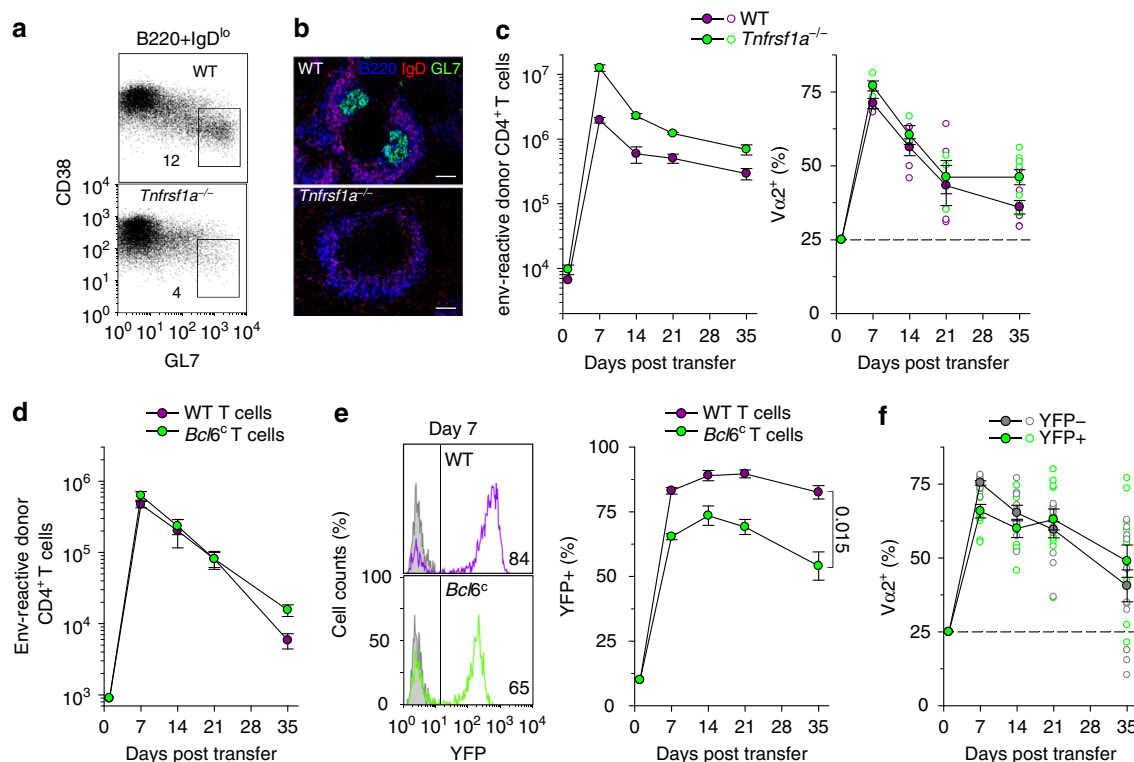


Figure 5 | Clonal replacement in virus-specific CD4⁺ T cells independently of Bcl6-dependent Tfh differentiation or germinal center reaction.

(a) Frequency of germinal center-phenotype (CD38^{lo}GL7^{hi}) cells in CD19⁺IgD^{lo} splenic B cells 35 days after FV infection of WT or *Tnfrsf1a*^{-/-} mice ($n=3$). (b) Germinal center (B220⁺IgD⁻GL7⁺) presence in the spleen of the same mice in a. The scale bar is 250 μ m. (c) Absolute numbers (left) and $V\alpha 2$ composition (right) of env-reactive donor EF4.1 CD4⁺ T cells in the spleens of WT or *Tnfrsf1a*^{-/-} recipient mice after adoptive T-cell transfer and FV infection ($n=3-9$ mice per time point). (d) Absolute numbers of WT or *Bcl6*^c env-reactive donor EF4.1 CD4⁺ T cells, additionally carrying the *Tnfrsf4*^{Cre} and *Gt(ROSA)26Sor*^{YFP} alleles, in the spleens of recipient mice after adoptive T-cell transfer and FV infection ($n=3-9$ mice per time point). (e) YFP expression on day 7 (left) and frequency of YFP⁺ cells over time (right) in the same env-reactive donor EF4.1 CD4⁺ T cells as in d. (f) $V\alpha 2$ frequency in YFP⁺ and YFP⁻ *Bcl6*-conditional env-reactive donor EF4.1 CD4⁺ T cells as in d. In c-f, closed symbols are the means (\pm s.e.m.); open symbols are individual mice.

exhibited typical response kinetics upon transfer into FV-infected hosts (Fig. 5d). However, the frequency of YFP⁺ cells in virus-specific donor CD4⁺ T cells was significantly lower in EF4.1 CD4⁺ T cells with the *Bcl6*^c than the WT allele (Fig. 5e), indicating that *Bcl6* is required for the persistence of at least some virus-specific CD4⁺ T cells. Nevertheless, the clonotypic composition of YFP⁺ (*Bcl6*-deleted) virus-specific donor CD4⁺ T cells was comparable with that of the YFP⁻ fraction (Fig. 5f). Thus, preventing *Bcl6*-dependent Tfh differentiation did not prevent the switch from $V\alpha 2$ to $V\alpha 3$ clonotypes ($P=0.016$, Mann-Whitney rank sum test).

These findings argued against the possibility that clonotypic replacement of $V\alpha 2$ clonotypes with *Traj31*-using $V\alpha 3$ clonotypes over the course of FV infection was owing to selective differentiation into the Tfh subset, whose long-term stability may differ from that of other Th subsets. This led us to consider an alternative hypothesis: instead of all virus-specific clonotypes engaging synchronously and *Traj31*-using $V\alpha 3$ clonotypes surviving longer than other clonotypes, it was possible that *Traj31*-using $V\alpha 3$ clonotypes were simply recruited with delayed kinetics.

Asynchronous expansion of high- and low-avidity clonotypes.

The extensive variability in the frequency of $V\alpha 3$ clonotypes between separate hosts during FV infection (Fig. 1b), and the 'private' nature of distinct *Traj31*-using $V\alpha 3$ clonotypes expanding in different hosts (Fig. 1c) hindered kinetic analyses of the deep-sequencing data. To establish conclusively the kinetics of

recruitment and expansion of a *Traj31*-using $V\alpha 3$ clonotype in response to FV infection, we transferred cohorts of allotypically marked monoclonal EV $\alpha 3$ T cells into WT hosts that were infected with FV or coinfecting with FV and LDV, either 10 days previously or on the day of T-cell transfer (Fig. 6a,b). EV $\alpha 3$ T cells transferred at the time of FV infection or FV/LDV coinfection expanded minimally 7 days later and became undetectable by day 21 post transfer (Fig. 6a,b). Also, EV $\alpha 3$ T cells transferred on day 10 of FV infection expanded modestly 7 days after transfer and contracted to low numbers thereafter (Fig. 6a,b). This pattern contrasted with strong expansion (>100-fold) of EV $\alpha 3$ T cells 7 days after transfer into hosts coinfecting with FV and LDV 10 days previously (Fig. 6a,b), when B-cell activation had peaked (Fig. 4a). For comparison, EF4.1T cells were also transferred into hosts that were coinfecting with FV and LDV, either 10 days previously or on the day of T-cell transfer, and maximal expansion of both $V\alpha 2$ and $V\alpha 3$ clonotypes was already observed the first 7 days of infection (Fig. 6c). These results demonstrated that EV $\alpha 3$ T cells were recruited later than higher-avidity virus-specific clonotypes and only in conditions where B cells were activated.

Later recruitment, as opposed to longer survival, of EV $\alpha 3$ T cells further argued that B-cell presentation did not necessarily instill qualitative differences in CD4⁺ T-cell clonotypes, but rather expanded the number of available APCs to the point where clonotypic competition was alleviated and lower-avidity T-cell clonotypes could be expanded. Indeed, recruitment and expansion of lower-avidity T-cell clonotypes depended on the

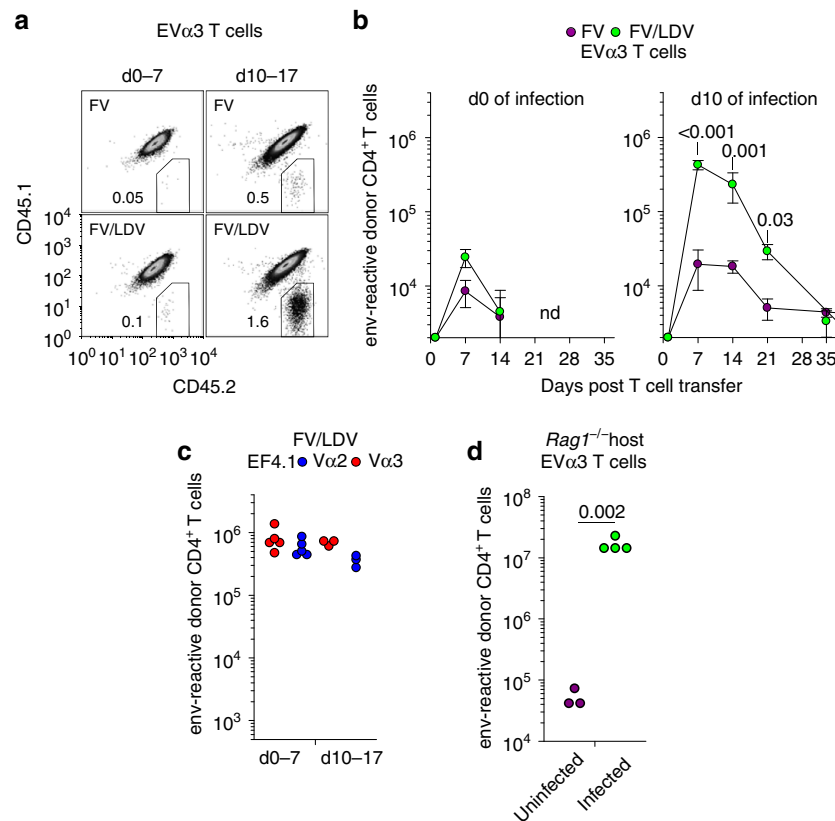


Figure 6 | Asynchronous expansion of higher- and lower-avidity clonotypes. (a) Flow cytometric detection of CD45.2⁺ donor EV α 3 Rag1^{-/-} Ems2^{-/-} CD4⁺ T cells and CD45.1⁺CD45.2⁺ host CD4⁺ T cells following transfer either on the day of infection (d0 of infection, d0-7) or 10 days after infection (d10 of infection, d10-17) with FV or FV/LDV. In both setups, T-cell expansion was analysed 7 days after transfer ($n=5-9$). (b) Absolute number of env-reactive donor EV α 3 CD4⁺ T cells recovered from the spleens of the same recipients described in a over the course of FV infection or FV/LDV coinfection (nd, not detected). (c) Absolute number of V α 2 or V α 3 env-reactive donor EF4.1 CD4⁺ T cells recovered from the spleens of FV/LDV infected recipients 7 days after transfer either on the day of infection (d0-7) or 10 days after infection (d10-17). (d) Numbers of EV α 3 T cells recovered 7 days after transfer from the spleens of lymphocyte-deficient Rag1^{-/-} Ems2^{-/-} recipients that were either left uninfected or were F-MLV-B-infected. Each symbol represents an individual mouse.

availability of activated B cells only in the presence of higher-avidity T-cell competitors. In contrast to their lack of expansion in FV-infected WT host (Fig. 6a,b), EV α 3 T cells expanded markedly when transferred into FV-infected Rag1^{-/-} hosts (Fig. 6d). These results were consistent with a quantitative, rather than qualitative effect of B-cell presentation on the expansion of lower-avidity CD4⁺ T-cell clonotypes, whereby the B-cell response gradually increases APC availability, which progressively recruits lower-avidity T-cell clonotypes, thus diversifying the CD4⁺ T-cell response.

B cells promote TCR diversity in various T-cell responses.

Our model would also predict that following infections or immunizations where B cells are dominant APCs, lower-avidity clonotypes would be induced, in addition to higher-avidity clonotypes. To test this prediction, we compared the dependence on B cells of EF4.1 CD4⁺ T-cell priming by the replication-attenuated F-MLV-N vaccine virus and fully competent FV, which induce lower- and higher-avidity responses, respectively (Fig. 1b and Fig. 3c). Indeed, CD4⁺ T-cell priming by F-MLV-N, but not FV, was significantly compromised in the absence of B cells (Fig. 7a). Similarly, priming with a replication-defective human Adenovirus 5 (Ad5)-based vector, expressing F-MLV gp70 (Ad5.pIX-gp70), which has previously found to induce primarily lower-avidity responses¹⁶, was also compromised in the

absence of B cells (Fig. 7a). Therefore, vaccines that rely on B-cell presentation induce lower-avidity CD4⁺ T-cell responses.

The applicability of this model was also tested in two additional immunization regimens. WT or *Ighm*^{-/-} hosts were challenged with FBL-3 cells, a FV-induced tumour cell line that expresses F-MLV gp70, but does not produce infectious viral particles³². Adoptively transferred EF4.1 CD4⁺ T cells responded with a high frequency of high-avidity V α 2 virus-specific CD4⁺ T-cell clonotypes in both types of host at peak (Fig. 7b). Importantly, this frequency remained significantly higher in *Ighm*^{-/-} than in WT hosts as the response progressed (Fig. 7b). Moreover, the clonotypic replacement of V α 2 virus-specific CD4⁺ T cells was observed following env₁₂₄₋₁₃₈ peptide immunization of WT, but not *Ighm*^{-/-} hosts, highlighting the requirement for B cells in the process. Thus, following either tumour challenge or peptide immunization, B cells were required for the full clonotypic diversity of the CD4⁺ T-cell response.

B cells balance TCR diversity during T-cell reconstitution.

Our model implied that B-cell presentation should promote TCR diversity not only in response to infection or immunization, but also in any setting where CD4⁺ T-cell clonotypic competition is likely to operate based on TCR avidity. To examine if this were the case, we monitored TCR repertoire skewing during CD4⁺ T-cell reconstitution of lymphopenic hosts, which selects distinct clonotypes according to TCR avidity. Hosts lacking only T cells

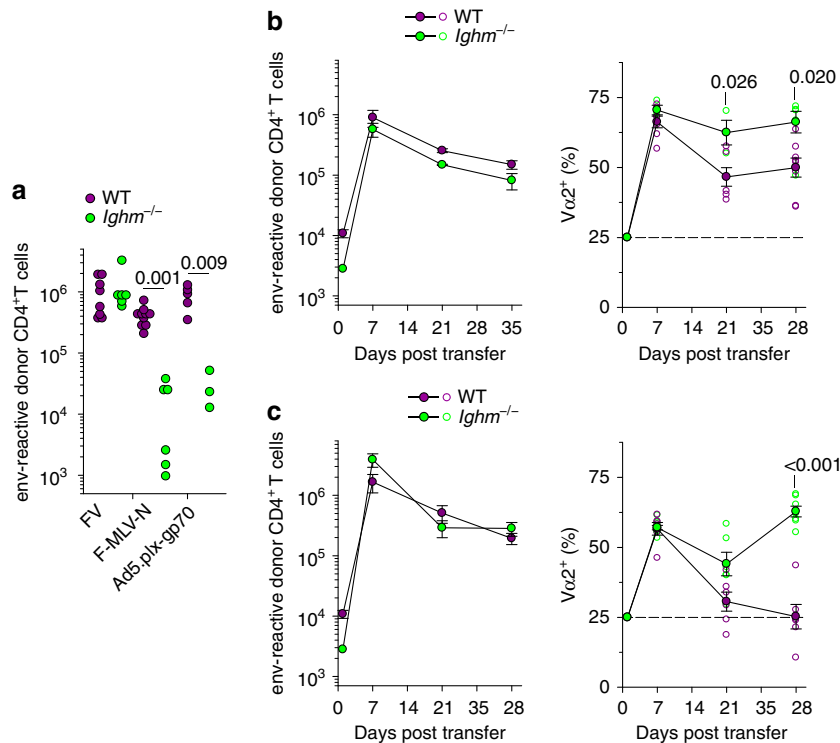


Figure 7 | B-cell-dependent expansion of lower-avidity CD4⁺ T-cell clonotypes in diverse infection or immunization settings. (a) Absolute number of env-reactive donor EF4.1 CD4⁺ T cells 7 days after transfer into WT or *Ighm*^{-/-} recipient mice infected either with FV or F-MLV-N or immunized with Ad5.pIX-gp70. Each symbol is an individual mouse. (b) Absolute numbers (left) and Vα composition (right) of env-reactive donor EF4.1 CD4⁺ T cells in the spleens of WT or *Ighm*^{-/-} recipient mice after adoptive T-cell transfer and FBL-3 tumor challenge (*n* = 3–8 mice per time point). (c) Absolute numbers (left) and Vα composition (right) of env-reactive donor EF4.1 CD4⁺ T cells in the spleens of WT or *Ighm*^{-/-} recipient mice after adoptive T-cell transfer and env₁₂₂₋₁₄₁ peptide immunization (*n* = 6–9 mice per time point).

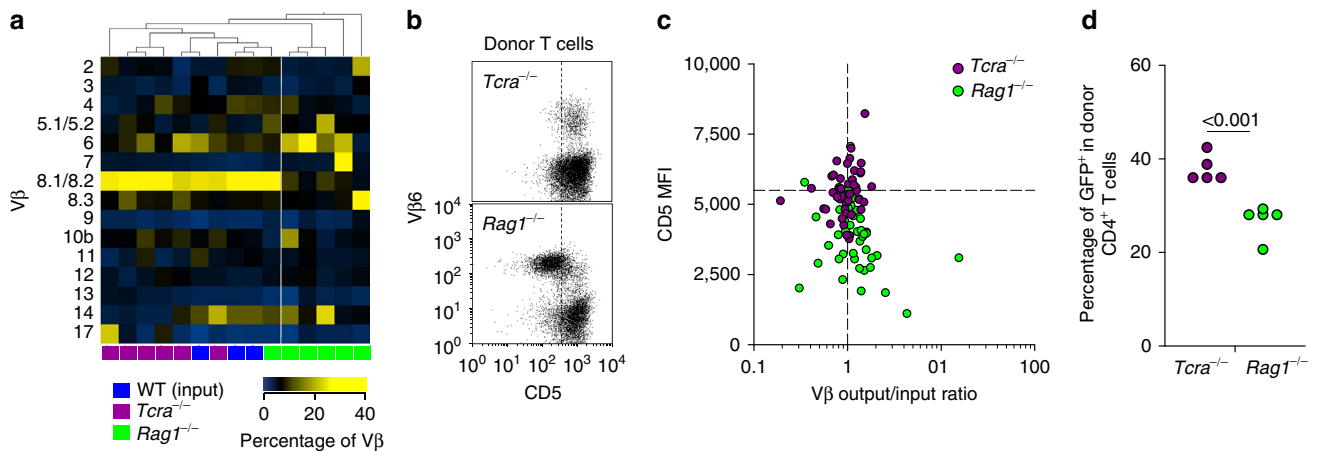


Figure 8 | Balanced TCR diversity during CD4⁺ T-cell reconstitution requires B cells. (a) Heat-map of hierarchically-clustered WT donors and *Tcra*^{-/-} or *Rag1*^{-/-} *Emv2*^{-/-} recipients of purified CD4⁺ T cells according to the frequency of the indicated Vβ family before (WT (input)) or 21 days after T-cell reconstitution (*Tcra*^{-/-} or *Rag1*^{-/-}). Each column is an individual mouse. (b) Flow cytometric detection of CD5 and Vβ6 expression in donor CD4⁺ T cells from the same recipients as in a. (c) CD5 median fluorescent intensity (MFI) plotted against the divergence from the input frequency of each detected Vβ family in donor CD4⁺ T cells from the same recipients as in a. Only three recipients are plotted for clarity. The horizontal dashed line represents the CD5 MFI in control cells (*P* < 0.001 between CD5 levels in T cells from the two types of host, Mann-Whitney rank sum test). (d) Frequency of GFP⁺ cells in donor CD4⁺ T cells 21 days after T-cell reconstitution of *Tcra*^{-/-} or *Rag1*^{-/-} *Emv2*^{-/-} (*Rag1*^{-/-}) recipients with purified CD4⁺ T cells from Nur77-GFP transgenic donors. Each symbol represents an individual mouse.

(*Tcra*^{-/-}) or both T and B cells (*Rag1*^{-/-}) were reconstituted by adoptive transfer of fully polyclonal purified CD4⁺ T cells and usage of different families of Vβ chains was compared between the input and expanded population in the respective host 21 days later (Fig. 8a). T-cell reconstitution of *Tcra*^{-/-} hosts preserved

the pattern of Vβ usage in the input population, as the two were indistinguishable by unsupervised clustering (Fig. 8a). In contrast, T-cell reconstitution of *Rag1*^{-/-} hosts resulted in considerable skewing in Vβ usage in 5 out of 6 such hosts, which clustered separately from all other hosts (Fig. 8a). TCR Vβ usage skewing

was not related to differences in overall T-cell reconstitution between *Tcra*^{-/-} and *Rag1*^{-/-} hosts, as it also characterized hosts with comparable numbers of expanded CD4⁺ T cells (Supplementary Fig. 4). TCR repertoire skewing in *Rag1*^{-/-} hosts was owing to 'private' expansion of distinct V β families in individual mice (Fig. 8a), suggestive of TCR driven responses. Moreover, levels of CD5 expression were significantly reduced in CD4⁺ T cells expanded in *Rag1*^{-/-} hosts in comparison with those expanded in *Tcra*^{-/-} hosts (Fig. 8b,c), indicating insufficient MHC II-derived signals in *Rag1*^{-/-} hosts^{33,34}. Indeed, use of the Nur77-GFP reporter for TCR signalling³⁵ revealed that CD4⁺ T cells received stronger overall TCR signals in *Tcra*^{-/-} than *Rag1*^{-/-} hosts (Fig. 8d), suggesting that B cells were necessary to provide CD4⁺ T cells with optimal TCR signal, which would be critical for the expansion of lower-avidity clonotypes. Thus, balanced representation of TCR clonotypes, at least at the level of distinct V β families during T-cell reconstitution, required B cells.

Discussion

Our findings highlight the prominent role for the TCR in setting the clonotypic hierarchy during the CD4⁺ T-cell response, suggested by studies in many systems³⁶. They lend support to the recent recognition of the importance of self-reactivity, rather than affinity for antigen, in determining the fate of CD4⁺ and CD8⁺ T cells during the response to foreign antigens^{11,12,37}. However, they further uncover the role of B-cell presentation as a powerful T-cell-extrinsic factor that can reverse TCR sensitivity-based hierarchies. Indeed, although T-cell clonal selection driven by TCR affinity for self or foreign antigens progressively narrows the responding TCR repertoire, B cells are critical in preserving diversity of the antigen-selected TCR repertoire.

The progression of the CD4⁺ T-cell response is generally expected to enrich for high-avidity clonotypes, accentuated by diminishing antigen levels, a notion that is supported by experimental data^{10,38–40}. The central importance of TCR signal strength in memory formation would gradually reduce the diversity to a few or theoretically the one clonotype with the highest avidity. However, enrichment for high-avidity clonotypes is not consistent with either continuous clonal replacement during chronic T-cell responses⁴¹ or following secondary responses^{10,42,43}. Moreover, memory CD4⁺ T-cell populations with lower overall avidity than the primary response have also been found in response to *Salmonella typhimurium* infection⁴⁴, and a mouse adenocarcinoma-associated antigen⁴⁵.

The contribution of low-avidity CD4⁺ T cells to the antigen-specific response may be underestimated owing to technical difficulties in detecting such clonotypes by pMHC II tetramers^{23,24}. Nevertheless, an equally plausible explanation for variable participation of lower-avidity CD4⁺ T-cell clonotypes is likely related to the nature of antigen and the range of TCR affinities it elicits. T-cell-extrinsic effects on TCR clonotypic composition will be particularly pronounced when TCR affinity for antigen might not be strong enough to overcome these effects. For example, self-tolerance is likely to reduce the overall avidity of T-cell responses to tumour-associated or self-antigens or to pathogen antigens with significant similarity with self, such as retroviruses^{1,2}.

Another important variable in studies of TCR repertoire changes over the course of the CD4⁺ T-cell response is the definition of the exact property of antigen-selected TCRs. Although there is general consensus that CD4⁺ T cells are selected on the basis of TCR signal strength in response to antigen, the underlying factors responsible for differences in TCR sensitivity are still a matter of debate. TCR binding kinetics to

antigenic pMHC II complexes have traditionally been considered as the dominant factor^{9,46}. However, the importance of TCR self-reactivity in setting TCR responsiveness to antigen is increasingly appreciated^{11,12,37}. Strong self-reactivity has been suggested to select for TCRs with improved binding kinetics to antigenic pMHC¹² or to maintain a more efficient state of TCR signalling capacity, irrespective of affinity to antigenic pMHC¹¹. Our results with the EV α 2 and EV α 3 TCRs are consistent with the latter notion, whereby differences in functional avidity and biological response correlate with self-reactivity rather than affinity to antigen¹¹. However, as a direct mechanistic link between self-reactivity and antigen sensitivity was not examined in the current study, our results do not prove that differences in antigen sensitivity are indeed caused by differences in self-reactivity.

Although naive CD4⁺ T-cell priming is thought to be initiated by DCs in the T-cell zone of secondary lymphoid organs, the contribution to maximal T-cell expansion of additional APCs and B cells in particular, is well-recognized⁴⁷. Our findings uncover an additional dimension to the antigen-presenting contribution of B cells, namely the dependence on the B-cell response itself. Indeed, B-cell-mediated expansion of lower-avidity CD4⁺ T-cell clonotypes was proportional to the degree of B-cell activation. Polyclonal B-cell activation is a feature of many viral infections or autoimmune diseases^{48,49}. Notably, progression of human immunodeficiency virus-1 infection is characterized by stepwise B-cell hyperactivation⁵⁰, asynchronous expansion of CD8⁺ T cells specific to distinct epitopes⁵¹ and increase in virus-specific CD4⁺ T cells with low functional avidity⁵². The observation that germinal center formation was redundant in this process and that expansion of lower-avidity CD4⁺ T-cell clonotypes correlated simply with the overall number of activated B cells in bone marrow chimeras, argue against a requirement for a specific B-cell subset. Moreover, efficient priming of lower-avidity CD4⁺ T-cell clonotypes in the absence of B cells, when higher-avidity T-cell competitors were also absent, further argues against a unique type of antigen presentation by B cells. Instead, these findings suggest that B cells, which outnumber DCs at steady-state by two orders of magnitude⁵³ and which further expand in response to polyclonal and antigen-specific stimuli during infection, provide the necessary abundance of antigenic stimulation to allow priming and expansion of all clonotypes irrespective of TCR avidity.

Our findings also indicate an essential role for B cells in maintenance of a diverse and balanced TCR repertoire during CD4⁺ T-cell reconstitution of lymphopenic hosts, typically driven by relatively low-avidity interactions with self- and environmental-antigens and selecting for clonotypes that receive the strongest TCR signal⁴. These results, thus, further support the idea that B cells facilitate the expansion of lower-avidity clonotypes in general. Similarly, B cells may be critically required to initiate CD4⁺ T-cell responses to an autoantigen, which would be typically low-avidity. Interestingly, non-obese diabetic mice do not develop autoimmunity if they are rendered deficient in B cells⁵⁴, and B-cell reconstitution is required for the formation of a diverse TCR repertoire of CD4⁺ T-cell infiltrating the pancreas⁵⁵. Although the overall avidity for pancreatic autoantigens of the different TCR repertoires was not examined⁵⁵, these studies offer further support to the notion that B cells increase the diversity of responding CD4⁺ T cells.

B cells have long been suspected as drivers of the diversification of the CD4⁺ T-cell response⁵⁶ and this study provides clear evidence of their involvement. In contrast to the intrinsic TCR affinity of distinct clonotypes and the clonotypic diversity in an individual, manipulating the degree of B-cell activation or antigen

presentation to CD4⁺ T cells, might provide a more amenable way of controlling the antigen-specific TCR repertoire during infection, vaccination or autoimmunity.

Methods

Mice. Inbred B6 and CD45.1⁺ congenic B6 (B6.SJL-*Ptprca*^d *Pep3*^h/BoyJ) mice were originally obtained from The Jackson Laboratory (Bar Harbor, ME, USA). TCRβ-transgenic EF4.1 mice²¹, Rag1-deficient (*Rag1*^{-/-}) mice⁵⁷, B-cell-deficient (*Ighm*^{-/-}) mice⁵⁸, SAP-deficient (*Sh2d1a*^{-/-}) mice⁵⁹, TCR α-deficient (*Tcrα*^{-/-}) mice⁶⁰, MHC II-deficient (*H2-Ab1*^{-/-}) mice⁶¹, TNF receptor I-deficient (*Tnfrsf1a*^{-/-}) mice⁶², mice with an activatable YFP gene targeted into *Gt(ROSA)26Sor (R26)* locus⁶³, mice with a targeted insertion of Cre recombinase into the *Tnfrsf4* locus⁶⁴ (*Tnfrsf4*^{Cre}), mice with a conditional *Bcl6* allele⁶⁵ (*Bcl6*^C), endogenous ecotropic MLV-deficient (*Emv2*^{-/-}) mice²³ and Nur77-GFP transgenic mice³⁵ were all on the B6 genetic background. TCRαβ-transgenic EVα2 and EVα3 mice were created by conventional transgenesis (Supplementary Fig. 5). Briefly, cDNAs encoding the TCRα and TCRβ chains of the H5 and H18 env-specific CD4⁺ T-cell clones, respectively, from the polyclonal repertoire of EF4.1 mice²³, were cloned and inserted into the hCD2-VA expression cassette²¹. Each of these constructs was mixed with a construct encoding the TCRβ chain of EF4.1 mice and integrated into the DNA of fertilized B6 oocytes following pronuclear microinjection. Transgenic founders were identified by flow cytometry and genotyping for the presence of the TCRα and TCRβ transgenes. These new transgenic mice were crossed to *Rag1*^{-/-} mice, to preclude rearrangement and subsequent expression of productive endogenous TCR genes. They were additionally rendered deficient in *Emv2*, a single germ-line integration of a MLV found in B6 mice, and free from any *Emv2*-derived infectious MLVs that spontaneously arise in immunodeficient mice and have the potential to affect MLV-specific T-cell development and subsequent response⁶⁶. Male or female mice were used in separate experiments and were gender-matched within experiments. Mice were used at 8–12 weeks of age, with the exception of neonatal infection, which was carried out on 1–2 day-old mice. All animal experiments were approved by the ethical committee of the Francis Crick institute, and conducted according to local guidelines and UK Home Office regulations under the Animals Scientific Procedures Act 1986 (ASPA).

Retroviral infection and immunization. The FV used in this study was a retroviral complex of a replication-competent B-tropic F-MLV and a replication-defective SFV. Stocks were propagated *in vivo* and prepared from the spleen of infected mice. A pool of 20 LDV-free BALB/c mice was infected with FV, spleens were isolated 12 days later and homogenized (10% w/v) in phosphate-buffered saline. Aliquots were frozen and were subsequently used for infection. Mice received an inoculum of ~1,000 spleen focus-forming units of FV by intravenous injection. Stocks of F-MLV-B and F-MLV-N helper viruses were grown in *Mus dunni* fibroblast cells. Mice received an inoculum of ~10⁴ infectious units of F-MLV by intravenous injection. Neonatal F-MLV infection was performed by administering an inoculum of ~4,000 infectious units of F-MLV-B to 1-day-old mice by intraperitoneal injection. All stocks were free of Sendai virus, Murine hepatitis virus, Parvoviruses 1 and 2, Reovirus 3, Theiler's murine encephalomyelitis virus, Murine rotavirus, Ectromelia virus, Murine cytomegalovirus, K virus, Polyomavirus, Hantaan virus, Murine norovirus, Lymphocytic choriomeningitis virus, Murine adenoviruses FL and K87, *Mycoplasma* sp. and LDV. For coinfection of FV and LDV, a similarly prepared stock of FV additionally containing LDV was also used⁸. For peptide immunization, mice received an intraperitoneal injection of a total of 12.5 nmol of synthetic env₁₂₄₋₁₃₈ peptide mixed in Sigma Adjuvant System. FBL-3 tumour challenge was carried out by intravenous injection of 3 × 10⁶ FBL-3 cells. Ad5.pIX-gp70 stocks were prepared at a titre of 9 × 10⁹ viral genomes per ml by infection of 293A cells¹⁶. Approximately 5 × 10⁸ Ad5.pIX-gp70 viral genomes per mouse were administered intravenously.

F-MLV copy number analysis. DNA copy numbers of F-MLV were determined by real-time quantitative PCR (qPCR) on DNA samples isolated from the spleen cell suspensions from infected mice, using primers specific to F-MLV env DNA (125 bp product): forward 5'-AAGTCTCCCCCGCCTCTA-3' and reverse 5'-AGTGCCTGGTAAGCTCCCTGT-3'. Signals were normalized for the amount of DNA used in the reactions based on amplification of the single-copy *Ifnr1* gene (150 bp product) with primers: forward 5'-AAGATGTGCTGTTCCTTCC TCTGCTCTGA-3' and reverse 5'-ATTATTAAGAAAAGACGAGGCGA AGTGG-3'. Copy numbers were calculated with a ΔΔC_T method and are expressed as copies per million cells.

T-cell purification and adoptive transfer. Single-cell suspensions were prepared from the spleens and lymph nodes of donor CD45.1⁺ or CD45.2⁺ mice and CD4⁺ T cells were enriched using immunomagnetic positive selection (StemCell Technologies), at >96% purity. A total of 1 × 10⁶ CD4⁺ T cells were injected into CD45.1⁺CD45.2⁺ recipients via the tail vein. Where indicated, enriched EF4.1

CD4⁺ T cells were further purified (>98% purity) by cell sorting, performed on MoFlo cell sorters (Dako-Cytomation, Fort Collins, CO, USA).

Bone marrow chimeras. Bone marrow cell suspensions were prepared by flushing the bone cavities of femurs and tibiae from donor mice with air-buffered Iscove's Modified Dulbecco's Media. MHC II-sufficient or -deficient bone marrow cells were injected separately into non-irradiated *Ighm*^{-/-} recipients. In this setting, only the missing lymphocyte population (B cells) is reconstituted³¹, creating B-cell-specific loss of MHC II. Each recipient received between 1 × 10⁷ and 3 × 10⁷ bone marrow cells. Mice were bled for assessment of reconstitution and were used for infection 8–10 weeks post bone marrow transfer.

Flow cytometry. Single-cell suspensions were stained with directly conjugated antibodies to surface markers (Supplementary Table 1), obtained from eBiosciences (San Diego, CA, USA), CALTAG/Invitrogen, BD Biosciences (San Jose, CA, USA) or BioLegend (San Diego, CA, USA). Peptide-MHC II tetramers were prepared and used as previously described¹⁶. Multi-color cytometry were performed on Canto II, LSRFortessa X-20 (both from BD Biosciences) and CyAn (Dako) flow cytometers, and analysed with FlowJo v10 (Tree Star, Ashland, OR, USA) or Summit v4.3 (Dako) analysis software.

Micropipette adhesion frequency assay. Two-dimensional TCR affinities were measured by a micropipette adhesion frequency assay as has been described in detail elsewhere^{24,25}, using the T-cell hybridomas H5 and H18 and A^b-env₁₂₅₋₁₃₅ tetramer. Cells were brought into contact 50 times with the same contact time and area (A_c), and an adhesion frequency (P_a) was calculated. Surface pMHC and TCRβ densities were determined by flow cytometry and BD QuantiBRITE PE Beads for standardization (BD Biosciences). These parameters were then used to calculate two-dimensional affinity using the following equation: $A_c \times K_a = -\ln[1 - P_a(\infty)] m_1^{-1} m_2^{-1}$ where m_1 and m_2 represent TCR and pMHC surface densities, respectively.

In vitro T-cell activation. Spleen or lymph node single-cell suspensions were prepared from EF4.1 or EVα3 mice and 5 × 10⁵ cells per well were stimulated in 96-well plates with the indicated amount of the index env₁₂₂₋₁₄₁ epitope (DEPLTSLTPRCNTAWNRLKL), the shorter env_{124-138L} epitope (PLTSLTTPRCNTAWNRR) or the altered peptides epitopes env_{124-138Y} (PLTSYTPRCNTAWNRR) and env_{124-138I} (PLTSITTPRCNTAWNRR). Hybridoma cell lines were generated and stimulated as previously described²³. T-cell activation was assessed 18 h later by flow cytometric detection of CD69 or CD44 (eBiosciences).

Next-generation sequencing of the TCR repertoire. For TCR sequencing, naive or primed env-specific EF4.1 CD4⁺ T-cell subsets were purified by cell sorting (>98%) and RNA was isolated using the QIAcube (QIAGEN, Crawley, UK). Synthesis of cDNA was carried out with the High Capacity Reverse Transcription kit (Applied Biosystems, Carlsbad, CA, USA) with an added RNase-inhibitor (Promega Biosciences, Madison, WI, USA). A final clean-up was performed with the QIAquick PCR purification kit (Qiagen). Purified cDNA was then used as template for the amplification of *Trav14* (encoding Vα2)- or *Trav9* (encoding Vα3)-containing rearrangements, using the following primers: *Trav14* forward: 5'-CAAGCTTCAGCTAGGAGGAATGGAC-3'; *Trav9* forward: 5'-CCAAGGCTCAGCCATGCTCCTGGC-3'; *Trac* common reverse: 5'-TAACCTGGTACACAGCAGGTTCTGGG-3'. The forward *Trav*-specific primers were located in a promoter region common to all members of the respective *Trav* family and the common reverse was in the common constant region, thus amplifying the entire variable and joining coding region (~500 bp product). Between 4,500 and 43,000 sequences per sample (450 bp median size) were obtained on a GS FLX System by GATC Biotech (Constance, Germany). Identification of productive rearrangements, *Trav* and *Traj* gene segment annotation and protein translation and CDR3 segment prediction were performed by the ImMunoGeneTics (IMGT) online tool HighV-QUEST (<http://www.imgt.org>)⁶⁷.

Immunohistochemistry. Frozen OCT (Dako)-embedded spleen sections were fixed in cold acetone, stained with directly conjugated monoclonal antibodies (Supplementary Table 1) against B220 (AlexaFluor 647, BD Biosciences) and IgD (PE, eBiosciences). Sections were also stained for the T- and B-cell activation antigen Ly77 (clone GL7, FITC, BD Biosciences) and FITC fluorescence was amplified with the AlexaFluor 488 signal amplification kit (Molecular Probes), according to manufacturer's instructions. Stained sections were mounted in fluorescent mounting medium (Dako) and viewed with a Leica TCS SP2 AOBs confocal microscope. The images were acquired with Leica confocal software using the 20 × or 40 × objective lenses.

Statistical analyses. Statistical comparisons were made using SigmaPlot 12.0 (Systat Software, Germany). Parametric comparisons of normally distributed

values that satisfied the variance criteria were made by unpaired Student's *t*-tests. Data that did not pass the variance test were compared with non-parametric two-tailed Mann–Whitney rank sum test. Comparison of V β family expression, hierarchical clustering and heat-map production was with Qlucore Omics Explorer (Qlucore, Lund, Sweden).

References

- Turner, S. J., Doherty, P. C., McCluskey, J. & Rossjohn, J. Structural determinants of T-cell receptor bias in immunity. *Nat. Rev. Immunol.* **6**, 883–894 (2006).
- Sritesky, G. L., Jameson, S. C. & Hogquist, K. A. Selection of self-reactive T cells in the thymus. *Annu. Rev. Immunol.* **30**, 95–114 (2012).
- Thorborn, G., Young, G. R. & Kassiotis, G. Effective T helper cell responses against retroviruses: are all clonotypes equal? *J. Leukoc. Biol.* **96**, 27–37 (2014).
- Morris, G. P. & Allen, P. M. How the TCR balances sensitivity and specificity for the recognition of self and pathogens. *Nat. Immunol.* **13**, 121–128 (2012).
- Gett, A. V., Sallusto, F., Lanzavecchia, A. & Geginat, J. T cell fitness determined by signal strength. *Nat. Immunol.* **4**, 355–360 (2003).
- Fasso, M. *et al.* T cell receptor (TCR)-mediated repertoire selection and loss of TCR β diversity during the initiation of a CD4(+) T cell response *in vivo*. *J. Exp. Med.* **192**, 1719–1730 (2000).
- Malherbe, L., Hausl, C., Teyton, L. & McHeyzer-Williams, M. G. Clonal selection of helper T cells is determined by an affinity threshold with no further skewing of TCR binding properties. *Immunity* **21**, 669–679 (2004).
- Ploquin, M. J., Eksmond, U. & Kassiotis, G. B cells and TCR avidity determine distinct functions of CD4+ T cells in retroviral infection. *J. Immunol.* **187**, 3321–3330 (2011).
- Kim, C., Wilson, T., Fischer, K. F. & Williams, M. A. Sustained interactions between T cell receptors and antigens promote the differentiation of CD4(+) memory T cells. *Immunity* **39**, 508–520 (2013).
- Weber, K. S. *et al.* Distinct CD4+ helper T cells involved in primary and secondary responses to infection. *Proc. Natl Acad. Sci. USA* **109**, 9511–9516 (2012).
- Persaud, S. P., Parker, C. R., Lo, W. L., Weber, K. S. & Allen, P. M. Intrinsic CD4(+) T cell sensitivity and response to a pathogen are set and sustained by avidity for thymic and peripheral complexes of self peptide and MHC. *Nat. Immunol.* **15**, 266–274 (2014).
- Mandl, J. N., Monteiro, J. P., Vrsekooop, N. & Germain, R. N. T cell-positive selection uses self-ligand binding strength to optimize repertoire recognition of foreign antigens. *Immunity* **38**, 263–274 (2013).
- Tabo, N. J. *et al.* Single naive CD4(+) T cells from a diverse repertoire produce different effector cell types during infection. *Cell* **153**, 785–796 (2013).
- Malherbe, L., Mark, L., Fazilleau, N., McHeyzer-Williams, L. J. & McHeyzer-Williams, M. G. Vaccine adjuvants alter TCR-based selection thresholds. *Immunity* **28**, 698–709 (2008).
- Baumgartner, C. K., Yagita, H. & Malherbe, L. P. A TCR affinity threshold regulates memory CD4 T cell differentiation following vaccination. *J. Immunol.* **189**, 2309–2317 (2012).
- Thorborn, G. *et al.* Clonotypic composition of the CD4+ T cell response to a vectored retroviral antigen is determined by its speed. *J. Immunol.* **193**, 1567–1577 (2014).
- Rees, W. *et al.* An inverse relationship between T cell receptor affinity and antigen dose during CD4(+) T cell responses *in vivo* and *in vitro*. *Proc. Natl Acad. Sci. USA* **96**, 9781–9786 (1999).
- Anderton, S. M., Radu, C. G., Lowrey, P. A., Ward, E. S. & Wraith, D. C. Negative selection during the peripheral immune response to antigen. *J. Exp. Med.* **193**, 1–11 (2001).
- Hasenkrug, K. J. & Chesebro, B. Immunity to retroviral infection: the Friend virus model. *Proc. Natl Acad. Sci. USA* **94**, 7811–7816 (1997).
- Tsuiji-Kawahara, S. *et al.* Differential requirements of cellular and humoral immune responses for Fv2-associated resistance to erythroleukemia and for regulation of retrovirus-induced myeloid leukemia development. *J. Virol.* **87**, 13760–13774 (2013).
- Antunes, I. *et al.* Retrovirus-specificity of regulatory T cells is neither present nor required in preventing retrovirus-induced bone marrow immune pathology. *Immunity* **29**, 782–794 (2008).
- Kearney, E. R., Pape, K. A., Loh, D. Y. & Jenkins, M. K. Visualization of peptide-specific T cell immunity and peripheral tolerance induction *in vivo*. *Immunity* **1**, 327–339 (1994).
- Young, G. R. *et al.* Negative selection by an endogenous retrovirus promotes a higher-avidity CD4+ T cell response to retroviral infection. *PLoS Pathog.* **8**, e1002709 (2012).
- Sabatino, Jr. J. J., Huang, J., Zhu, C. & Evavold, B. D. High prevalence of low affinity peptide-MHC II tetramer-negative effectors during polyclonal CD4+ T cell responses. *J. Exp. Med.* **208**, 81–90 (2011).
- Huang, J. *et al.* The kinetics of two-dimensional TCR and pMHC interactions determine T-cell responsiveness. *Nature* **464**, 932–936 (2010).
- Kassiotis, G., Zamoyska, R. & Stockinger, B. Involvement of avidity for major histocompatibility complex in homeostasis of naive and memory T cells. *J. Exp. Med.* **197**, 1007–1016 (2003).
- Martin, B. *et al.* Highly self-reactive naive CD4 T cells are prone to differentiate into regulatory T cells. *Nat. Commun.* **4**, 2209 (2013).
- Dittmer, U., Brooks, D. M. & Hasenkrug, K. J. Characterization of a live-attenuated retroviral vaccine demonstrates protection via immune mechanisms. *J. Virol.* **72**, 6554–6558 (1998).
- Marques, R. *et al.* B lymphocyte activation by coinfection prevents immune control of Friend virus infection. *J. Immunol.* **181**, 3432–3440 (2008).
- Qi, H., Cannons, J. L., Klauschen, F., Schwartzberg, P. L. & Germain, R. N. SAP-controlled T-B cell interactions underlie germinal centre formation. *Nature* **455**, 764–769 (2008).
- Marques, R. *et al.* Generalized immune activation as a direct result of activated CD4+ T cell killing. *J. Biol.* **8**, 93 (2009).
- Klarnet, J. P. *et al.* FBL-reactive CD8+ cytotoxic and CD4+ helper T lymphocytes recognize distinct Friend murine leukemia virus-encoded antigens. *J. Exp. Med.* **169**, 457–467 (1989).
- Smith, K. *et al.* Sensory adaptation in naive peripheral CD4 T cells. *J. Exp. Med.* **194**, 1253–1261 (2001).
- Kassiotis, G., Garcia, S., Simpson, E. & Stockinger, B. Impairment of immunological memory in the absence of MHC despite survival of memory T cells. *Nat. Immunol.* **3**, 244–250 (2002).
- Moran, A. E. *et al.* T cell receptor signal strength in Treg and iNKT cell development demonstrated by a novel fluorescent reporter mouse. *J. Exp. Med.* **208**, 1279–1289 (2011).
- Hogquist, K. A. & Jameson, S. C. The self-obsession of T cells: how TCR signaling thresholds affect fate 'decisions' and effector function. *Nat. Immunol.* **15**, 815–823 (2014).
- Fulton, R. B. *et al.* The TCR's sensitivity to self peptide-MHC dictates the ability of naive CD8(+) T cells to respond to foreign antigens. *Nat. Immunol.* **16**, 107–117 (2015).
- McHeyzer-Williams, M. G. & Davis, M. M. Antigen-specific development of primary and memory T cells *in vivo*. *Science* **268**, 106–111 (1995).
- Savage, P. A., Boniface, J. J. & Davis, M. M. A kinetic basis for T cell receptor repertoire selection during an immune response. *Immunity* **10**, 485–492 (1999).
- Kim, C., Jay, D. C. & Williams, M. A. Stability and function of secondary Th1 memory cells are dependent on the nature of the secondary stimulus. *J. Immunol.* **189**, 2348–2355 (2012).
- Miconnet, I. *et al.* Large TCR diversity of virus-specific CD8 T cells provides the mechanistic basis for massive TCR renewal after antigen exposure. *J. Immunol.* **186**, 7039–7049 (2011).
- Buchholz, V. R. *et al.* Disparate individual fates compose robust CD8+ T cell immunity. *Science* **340**, 630–635 (2013).
- Gerlach, C. *et al.* Heterogeneous differentiation patterns of individual CD8+ T cells. *Science* **340**, 635–639 (2013).
- Ertelt, J. M. *et al.* Selective culling of high avidity antigen-specific CD4+ T cells after virulent *Salmonella* infection. *Immunology* **134**, 487–497 (2011).
- Caserta, S., Kleczkowska, J., Mondino, A. & Zamoyska, R. Reduced functional avidity promotes central and effector memory CD4 T cell responses to tumor-associated antigens. *J. Immunol.* **185**, 6545–6554 (2010).
- McHeyzer-Williams, L. J., Panus, J. F., Mikszta, J. A. & McHeyzer-Williams, M. G. Evolution of antigen-specific T cell receptors *in vivo*: preimmune and antigen-driven selection of preferred complementarity-determining region 3 (CDR3) motifs. *J. Exp. Med.* **189**, 1823–1838 (1999).
- Lund, F. E. & Randall, T. D. Effector and regulatory B cells: modulators of CD4(+) T cell immunity. *Nat. Rev. Immunol.* **10**, 236–247 (2010).
- Dorner, T., Giesecke, C. & Lipsky, P. E. Mechanisms of B cell autoimmunity in SLE. *Arthritis Res. Ther.* **13**, 243 (2011).
- Haas, A., Zimmermann, K. & Oxenius, A. Antigen-dependent and -independent mechanisms of T and B cell hyperactivation during chronic HIV-1 infection. *J. Virol.* **85**, 12102–12113 (2011).
- Moir, S. & Fauci, A. S. B cells in HIV infection and disease. *Nat. Rev. Immunol.* **9**, 235–245 (2009).
- Turnbull, E. L. *et al.* Kinetics of expansion of epitope-specific T cell responses during primary HIV-1 infection. *J. Immunol.* **182**, 7131–7145 (2009).
- Vingert, B. *et al.* HIV controller CD4+ T cells respond to minimal amounts of Gag antigen due to high TCR avidity. *PLoS Pathog.* **6**, e1000780 (2010).
- Waskow, C. *et al.* The receptor tyrosine kinase Flt3 is required for dendritic cell development in peripheral lymphoid tissues. *Nat. Immunol.* **9**, 676–683 (2008).
- Serreze, D. V. *et al.* B lymphocytes are essential for the initiation of T cell-mediated autoimmune diabetes: analysis of a new 'speed congenic' stock of NOD.Ig mu null mice. *J. Exp. Med.* **184**, 2049–2053 (1996).
- Vong, A. M. *et al.* Spectratyping analysis of the islet-reactive T cell repertoire in diabetic NOD Igm null mice after polyclonal B cell reconstitution. *J. Transl. Med.* **9**, 101 (2011).
- Mamula, M. J. & Janeway, Jr. C. A. Do B cells drive the diversification of immune responses? *Immunol. Today* **14**, 151–152 (1993).

57. Mombaerts, P. *et al.* RAG-1-deficient mice have no mature B and T lymphocytes. *Cell* **68**, 869–877 (1992).
58. Kitamura, D., Roes, J., Kuhn, R. & Rajewsky, K. A B cell-deficient mouse by targeted disruption of the membrane exon of the immunoglobulin mu chain gene. *Nature* **350**, 423–426 (1991).
59. Wu, C. *et al.* SAP controls T cell responses to virus and terminal differentiation of TH2 cells. *Nat. Immunol.* **2**, 410–414 (2001).
60. Philpott, K. L. *et al.* Lymphoid development in mice congenitally lacking T cell receptor alpha beta-expressing cells. *Science* **256**, 1448–1452 (1992).
61. Cosgrove, D. *et al.* Mice lacking MHC class II molecules. *Cell* **66**, 1051–1066 (1991).
62. Rothe, J. *et al.* Mice lacking the tumour necrosis factor receptor 1 are resistant to TNF-mediated toxicity but highly susceptible to infection by *Listeria monocytogenes*. *Nature* **364**, 798–802 (1993).
63. Srinivas, S. *et al.* Cre reporter strains produced by targeted insertion of EYFP and ECFP into the ROSA26 locus. *BMC. Dev. Biol.* **1**, 4 (2001).
64. Klinger, M. *et al.* Thymic OX40 expression discriminates cells undergoing strong responses to selection ligands. *J. Immunol.* **182**, 4581–4589 (2009).
65. Kaji, T. *et al.* Distinct cellular pathways select germline-encoded and somatically mutated antibodies into immunological memory. *J. Exp. Med.* **209**, 2079–2097 (2012).
66. Young, G. R. *et al.* Resurrection of endogenous retroviruses in antibody-deficient mice. *Nature* **491**, 774–778 (2012).
67. Alamyar, E., Duroux, P., Lefranc, M. P. & Giudicelli, V. IMGT(R) tools for the nucleotide analysis of immunoglobulin (IG) and T cell receptor (TR) V-(D)-J repertoires, polymorphisms, and IG mutations: IMGT/V-QUEST and IMGT/HighV-QUEST for NGS. *Methods Mol. Biol.* **882**, 569–604 (2012).

Acknowledgements

We wish to thank Dr Kristin A. Hogquist for the Nur77-GFP mice, Dr Toshitada Takemori for the conditional Bcl6 mice, Dr Kim Hasenkrug for FV and FBL-3 stocks, Dr Ulf Dittmer for the Ad5.pIX-gp70 stocks and Drs Anne O'Garra, Brigitta Stockinger, Mark Wilson and Eva Frickel for helpful comments and discussion. We are grateful for assistance from the Biological Services, Flow Cytometry and Protein Purification

Facilities at the Francis Crick institute. This work was supported by the Francis Crick Institute which receives its core funding from Cancer Research UK, the UK Medical Research Council (U117581330 to G.K.), and the Wellcome Trust.

Author contributions

J.M. performed and interpreted experiments and wrote the manuscript; M.J.P., U.E., G.T. and A.F. performed and interpreted experiments; R.A. and B.E. designed, performed and interpreted experiments relating to two-dimensional TCR affinity measurements. M.P. designed, prepared and provided the MHC II tetramer used in this study. G.K. designed and interpreted the experiments, wrote the manuscript and supervised the study.

Additional information

Accession codes: The Sequence Read Archive (SRA) and European Nucleotide Archive (ENA) accession numbers for the TCR sequences reported in this paper are SRX750575 and PRJEB11747, respectively.

Supplementary Information accompanies this paper at <http://www.nature.com/naturecommunications>

Competing financial interests: The authors declare no competing financial interests.

Reprints and permission information is available online at <http://npg.nature.com/reprintsandpermissions/>

How to cite this article: Merckenschlager, J. *et al.* Stepwise B-cell-dependent expansion of T helper clonotypes diversifies the T-cell response. *Nat. Commun.* **7**:10281 doi: 10.1038/ncomms10281 (2016).



This work is licensed under a Creative Commons Attribution 4.0 International License. The images or other third party material in this article are included in the article's Creative Commons license, unless indicated otherwise in the credit line; if the material is not included under the Creative Commons license, users will need to obtain permission from the license holder to reproduce the material. To view a copy of this license, visit <http://creativecommons.org/licenses/by/4.0/>